

## Mandrel-Free Bending of Tubes with Small Radii – A Theoretical and Experimental Study

Jacek Michalczyk<sup>1\*</sup>, Andrzej Gontarz<sup>2</sup>, Sylwia Wiewiórowska<sup>1</sup>, Grzegorz Winiarski<sup>2</sup>

<sup>1</sup> Department of Production Engineering and Materials Technology, Częstochowa University of Technology, Częstochowa, Poland

<sup>2</sup> Department of Mechanical Engineering, Lublin University of Technology, Lublin, Poland

\* Corresponding author's e-mail: [jacek.michalczyk@pcz.pl](mailto:jacek.michalczyk@pcz.pl)

### ABSTRACT

This paper presents the theoretical and experimental results of a study investigating a new method for tube bending. The method involves three-point bending of a tube without using a mandrel. The bending process was conducted with a small bending radius of  $R_g = 1.5D_z$  (where  $D_z$  is the outside diameter of the bent tube) and a large bending angle of  $180^\circ$ . The novelty of the proposed solution is the use of new shapes of bending roll impression. Instead of the standard circular-shaped impression, an elliptical-shaped impression was used. The aim of the study on the proposed small radius tube bending technique was to optimize the shape of roll impression in terms of minimizing ovalization and flattening of the tube cross section in the bending zone. Previous studies only showed that circular impressions were inefficient. The tube bending process conducted with a circular impression roll, without the use of a mandrel or other type of filling to achieve an angle ranging  $90^\circ \div 180^\circ$ , led to the flattening of the cross section. The tube wall in the upper zone would crack or its cross section would become deformed and oval. This theoretical and experimental study was conducted on tubes with an outside diameter of  $D_z = 20$  mm and a wall thickness of  $g = 2$  mm, made of 16Mo3 boiler steel and EN-AW 6060 aluminum alloy. Obtained results were then used to determine the ranges of bending roll impression parameters that ensured that the product would meet the standardized conditions of cross-sectional ovalization in the bending zone. The tool developed for this study can be applied in industrial practice.

**Keywords:** bending of tubes, mandrel-free bending, small bending radii, tube bending modeling.

### INTRODUCTION

Bending is a well-known and widely used method for cold forming of tubes and profiles described by Misiūnaitė [1] and other authors of paper [2, 3]. Tubes and profiles are deformed by rolls in bending machines. What they presented in the paper [4, 5] Ghiotti and Chung. As they showed in their article [6] Hermes and Zahn [7] tube bending process is relatively trouble-free. However, limitations arise when deformation requires small bending radii and large bending angles. We can speak of small bending radii when the following condition is met:  $1.5 D_z \leq R_g \leq 3.0 D_z$ , where  $R_g$  is the bending radius,  $D_z$  is the outside diameter of the tube.

Therefore, the bending methods used in industrial practice include mandrel bending and mandrel-free bending techniques.

Authors' article [8] Li and [9] Al-Qureshi show that mandrel bending is used for thin-walled tubes. In addition, the need for a mandrel occurs when small bending radii and large bending angles are used and it has been demonstrated in a scientific paper Xunzhong [10]. The mandrel is used to prevent the inward collapse of the bent tube wall. It prevents ovalization and flattening of the cross section as shown by the research in the authors' paper Simonetto [11] and Engel [12]. The roll impression on which the tube is bent is usually a semi-circle with a radius equal to the radius of the bent tube. In mandrel-free bending, the

tube can be pressed against the template with a roller or other elements. Research by Teheri et al [13] showed that Mandrel-free methods are used for bending thick-walled tubes and the authors of the study in paper Hermes et al [14] confirmed such results. Heng [16] showed in his study that key parameters affecting the use of a given method are the relative wall thickness, as well as bending radius and angle. The difficulty of performing a bending operation is greater when the bending radius and wall thickness are smaller as discussed in the paper [17] by Diamaluddin et al. Since bent tubes are also structural components, requirements are imposed on their strength and aesthetics. The dimensions and shape of the internal cross section, commonly known as the light or clearance, are very important. They determine the fluid flow capacity inside the tube. Examples of use for such tubes include heat exchangers, transmission systems and hydraulic systems in machinery and transportation equipment (aircraft). This was discussed in detail by the authors of the paper [18].

The basic criteria for evaluating a bent tube include:

- ovalization of the tube cross section at the point of greatest flattening,
- thinning of the wall,
- wrinkling of the bent cross section.

When studying the problem of mandrel-free bending of tubes using small radii, the authors of the paper [19] discovered that a change in the shape of the roll impression caused changes in the ovalization of the tube cross section in the bending zone. It was proposed that the main aim of this study would be to determine the influence of roll impression shape on the ovalization of the tube cross section in the bending zone. Based on preliminary numerical calculations, it was concluded that a non-circular or near-circular shape should be used. It was noted that the use of a parabolic impression shape caused the opposite effect, i.e. it led to an increased wall collapse above the neutral axis.

A review of the literature and preliminary studies showed the need for undertaking research on the optimization of tool shape in mandrel-free bending of tubes with round cross sections. The purpose of this study was to develop the bending roll impression shape that would ensure the lowest distortion of the tube cross section in the bending zone.

## MATERIALS AND RESEARCH METHODS FOR NUMERICAL ANALYSIS

In a study [2], the authors Michalczyk and Wojsyk performed numerical simulations of a tube bending process using small radii, which had the character of a preliminary analysis. The numerical program Forge®3D was used to that end. The program performs calculations by the finite element method (FEM). Tetragonal finite elements were used. The tetragonal mesh is effective for forming parts with thicknesses of more than 2.5 mm.

Simufact has options for overlaying a square finite element mesh. The dedicated mesh is for thin-walled elements. It works well for roving and bending. It speeds up calculations and there are no calculation errors during remeshing. For thin-walled elements of 2 mm and less, the FEM mesh can be compacted locally and more elements can be obtained than for tetragonal mesh.

Given that tube bending problems occur for thin-walled components, tubes with an outside diameter of 20 mm and a wall thickness of 2 mm were investigated. In this study, the numerical modeling of a tube bending process was performed using the Simufact Forming software, which allows deforming thin-walled parts with the use of rectangular sheet mesh finite elements. The numerical simulations of the bending process were carried out with a bending roll feed rate of  $V_g = 2$  mm/s and the Coulomb friction model ( $\mu = 0.15$ ) was used. It was the small contact area between tool and pipe and oil lubrication.

In this theoretical and experimental study, tubes were made of two materials: EN-AW 6060 aluminum alloy and 16Mo3 boiler steel.

The mesh elements are sheetmesh – element type (hexahedral). Three elements were used for the thickness of the pipe wall with a size of 0.7 mm. The number of elements is 84633. The mesh had a density in the bending (critical) area of 1. In Simufact software, this means that the mesh is twice as detailed. The FEM mesh rebuilding criterion was set as a strain change option. This means that mesh remeshing will start when the cumulative strain measure of any element reaches a limit starting from an undeformed mesh (or a new mesh after remeshing).

The EN-AW 6060 (AlMgSi) aluminum alloy has medium tensile strength and medium fatigue strength. This alloy can be decoratively anodized and welded. Its high deformability makes it possible to obtain profiles with complex shapes.

It is most often used in the production of aluminum bars and profiles. The EN-AW 6060 alloy is a good construction material and is used to make components of vehicles, ships, hydraulic systems, masts, etc. The correct performance of computer simulations of metal forming process depends on entering appropriate material data into the computer program. The EN-AW 6060 aluminum alloy is a widely used material with known rheological properties. Therefore, its properties were taken from the Simufact Forming material library database.

The Simufact computer program used an elastic-plastic model for calculations. For 16Mo3 aluminum alloy steel, the model was developed by the Simufact program writers on the basis of a ready-made equation for plastic stress. For EN-AW 6060 alloy, the model was developed on the basis of flow curves and approximation of strain rate data.

The chemical composition of EN-AW 6060 aluminum alloy is shown in Table 1.

The 16Mo3 steel grade is commonly referred to as boiler steel. It contains an increased molybdenum content and has a lower chromium content than, for example, 13CrMo-4-5 steel. This alloy contains a maximum of 0.3% Cr and 0.25–0.35%

Mo. 16Mo3 sheets and bars are suitable for machining and can be easily welded, and are formable and ductile at both low and high temperatures. 16Mo3 steel has good heat resistance. Steel of this grade is used primarily in the power industry. 16Mo3 steel can be a structural component of various devices, such as furnaces, pressure vessels of pipelines, devices for transporting hot liquids. Rheological data of the 16Mo3 boiler steel grade used for numerical modelling of small radius mandrel-free tube bending were taken from the Simufact Forming material library database. The chemical composition of the 16Mo3 steel is shown in Table 2.

In general, the materials selected for testing are widely used for the manufacture of structural and transmission components.

Previous studies on tube bending were theoretical and experimental. Therefore, numerical simulations and laboratory tests were conducted based on the same concept of bending roll impression geometry. The bending scheme for numerical modeling consisted of three-point bending of a tube at an angle of 180°. A CAD model of the bending machine is shown in Figure 1.

**Table 1.** Chemical composition of EN-AW 6060 aluminum alloy (AlMgSi) [20]

Si	Fe	Cu	Mn	Mg	Cr	Zn	Ti
0.30–0.6	0.10–0.30	≤0.10	≤0.10	0.35–0.60	0.03–0.06	0.10–0.15	≤0.10

**Table 2.** Chemical composition of 16Mo3 steel [21]

C	Mn	Si	P	S	Cr	Mo	Ni	Cu	N
0.12–0.20	0.40–0.90	≤0.35	≤0.025	≤0.010	≤0.30	0.25–0.35	≤0.30	≤0.30	≤0.012

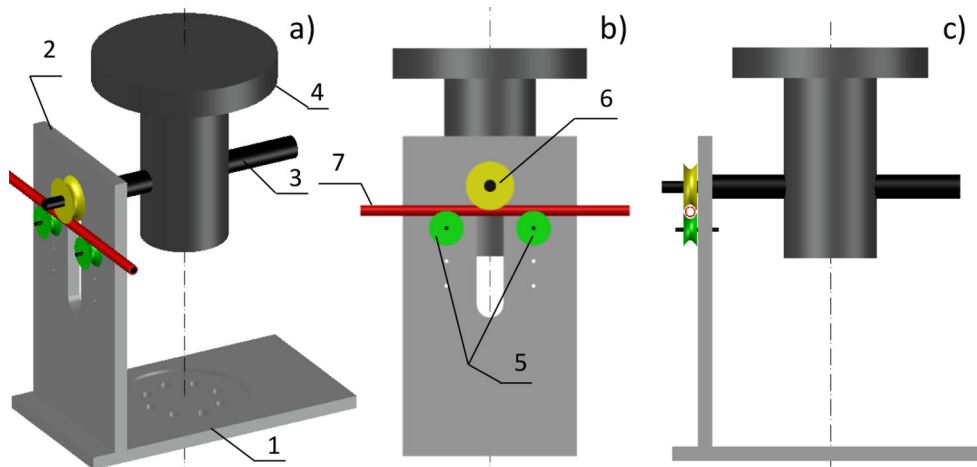


**Fig. 1.** CAD model of a bending machine: (a) isometric view, (b) front view, (c) side view; 1 – base plate, 2 – front plate, 3 – bending roll shaft, 4 – punch, 5 – support rollers, 6 – bending roll, 7 – tube

The bending machine consists of a base plate 1, a face plate 2 and a bending roll shaft 3 connected with a punch 4. Support rollers 5 are mounted to the front plate 2. The support rollers 5 can be moved horizontally. At the end of the bending roll shaft 3 a bending roller 6 is mounted. A tube 7 is placed on the support rollers 5.

The idea of developing a new technique for mandrel-free tube bending with small radii was to reduce ovalization of the cross section in the bending zone. Ovalization occurs as a result of thinning of the tube wall in the tension zone. The wall undergoes thinning and collapses. In the case of materials with low deformability, the tube wall in the bending zone cracks. As a result of the conducted research and analysis, a new impression shape of the bending roll was developed that minimizes the ovalization effect. In a further stage of the research, an optimal impression shape was determined to minimize ovalization for different materials.

For this reason, four variants of impressions were developed. The design of the first impression assumed a circular shape, which did not give the expected result. The design of the impression by which a positive result will be obtained is based on an elliptical shape. The purpose of the study was to demonstrate the reduction in the degree of ovalization of the cross

section of a bent tube that could be obtained with the new impression shape, when compared to the standard impression shape. Circular and elliptical impressions are formed by connecting points located on the circumference of the tube with the points located on the axis of tool symmetry. For a circular impression, this means connecting points 1-2-3-4-5-5', as shown in Figure 2 and Figure 3a.

The developed innovative impression has an elliptical shape. The elliptical curve for the first variant was created by connecting points 1-2-1',

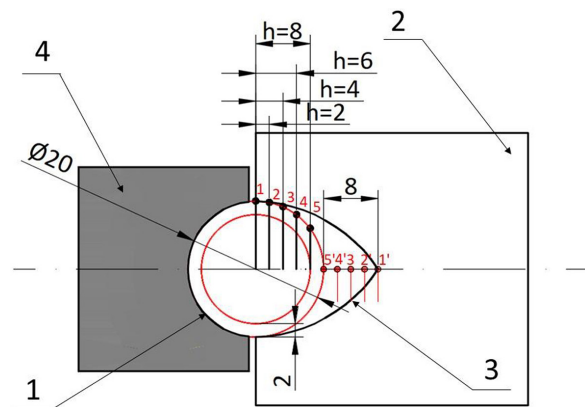


Fig. 2. Shape of the roll impression for small radius bending for a bending radius of  $1.5 Dz = Rg$  (1 – tube, 2 – bending roll, 3 – bending roll impression, 4 – support roller)

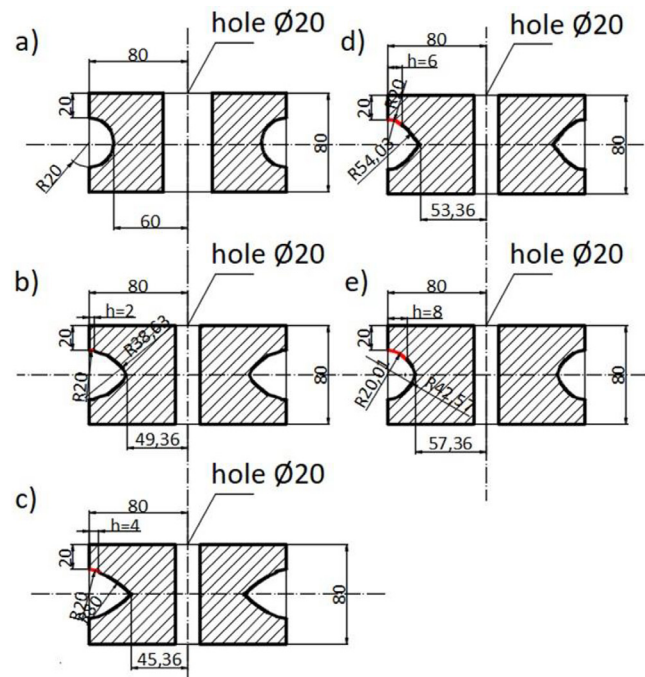


Fig. 3. Bending roll impressions for numerical modeling and laboratory tests with tube insertion depths: (a) circular impression, (b) elliptical impression,  $h = 2$  mm, (c) elliptical impression  $h = 4$  mm, (d) elliptical impression  $h = 6$  mm, (e) elliptical impression  $h = 8$  mm

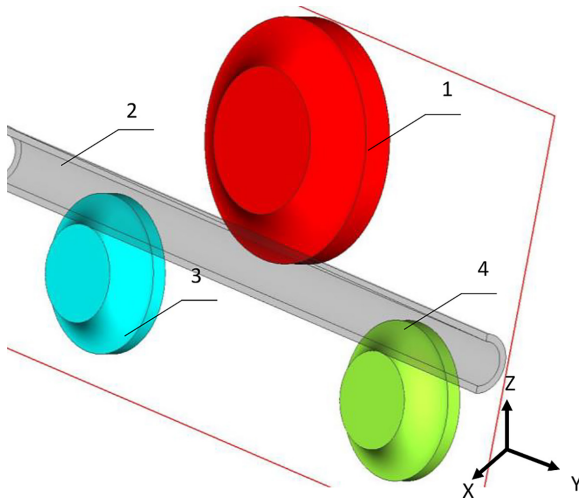


Fig. 4. 3D CAD model of tube bending process; 1 – bending roll, 2 – tube, 3, 4 – support rollers

as shown in Figure 2 and Figure 3b. The depth of tube insertion in the impression was determined by the parameter “h” and then made equal to  $h = 2$  mm. The second studied variant of impression was formed by connecting points 1-2-3-2’ with an elliptical curve (Fig. 2 and Fig. 3c). The tube was inserted into the impression at a depth of  $h = 4$  mm. The third variant of bending roll impression was obtained by connecting points 1-2-3-4-3’, (Fig. 2 and Fig. 3d) and inserting the tube at a depth of  $h = 6$  mm. The fourth and final variant of bending roll impression shape was created by connecting points 1-2-3-4-5-4’ by an elliptical line (Fig. 2 and Fig. 3e), and the tube insertion depth in the impression was  $h = 8$  mm.

Figures 3a–e show different variants of bending roll impressions employed in the numerical simulations and experiments.

The developed geometries of the bending roll impressions were used to build a 3D CAD process model, and this model was then implemented into the numerical simulation program Simufact Forming. The CAD model of the bending process for tube axial cross section is shown in Figure 4.

The aim of this study was to achieve the smallest possible cross-sectional ovalization of the tube in the bending zone. As a criterion for the evaluation of ovalization, the parameter “e” was adopted for determining the percentage of cross-sectional ovalisation. The formula for calculating ovalization was used from the authors’ article [22]. The formula works well for thick-walled pipes and the authors verified its performance experimentally.

$$e = \frac{D_{max} - D_{min}}{D_{max} + D_{min}} \cdot 100\% \quad (1)$$

where:  $D_{max}$  – the largest inside diameter of the tube after bending,

$D_{min}$  – the smallest inside diameter of the tube after bending. According to the PN-EN 12952-5 standard, the ovalization parameter should not exceed 12% for  $R_g \leq 2Dz$  and 8% for  $R_g > 2.5Dz$ .

Thus, the optimization consisted in determining the impression shape that would ensure the lowest value of the ovalization parameter e for the tested materials. The study also determined the range of values of the h parameter which would ensure the achievement of the ovalization parameter e satisfying the acceptable values specified under the standard.

## NUMERICAL ANALYSIS

Numerical simulations of the bending process performed using the Simufact Forming software were aimed at determining the effect of elliptical impression on the reduction of ovalization of the tube cross section. The study also aimed to select optimal shape of the bending roll impression, which means that the cross-sectional ovalization in the bending zone would have to be the lowest for this impression. The numerical simulations of the bending process were performed using two bending radii:  $R_g = 1.5Dz$  and  $R_g = 2.0Dz$ , where  $R_g$  is the bending radius,  $Dz$  is the outside diameter of the tube.

In order to demonstrate the influence of roll impression shape on the tube cross section in the bending zone, selected results of the numerical calculations for the EN-AW 6060 aluminum alloy ( $h = 2$  mm) and 16Mo3 steel ( $h = 8$  mm) samples are given below. Figures 5 and 6 show the selected simulation results of the bending process obtained for the EN-AW 6060 aluminum alloy sample.

The numerical simulations of the tube bending process (Figs. 5 a, b, c) conducted using a circular impression of the bending roll and a bending angle of  $180^\circ$  showed that the cross section collapsed and flattened (Fig. 5b). The top wall collapsed and the cross section became oval. The use of a non-circular shape of the roll impression (elliptical) with a tube insertion depth of 2 mm

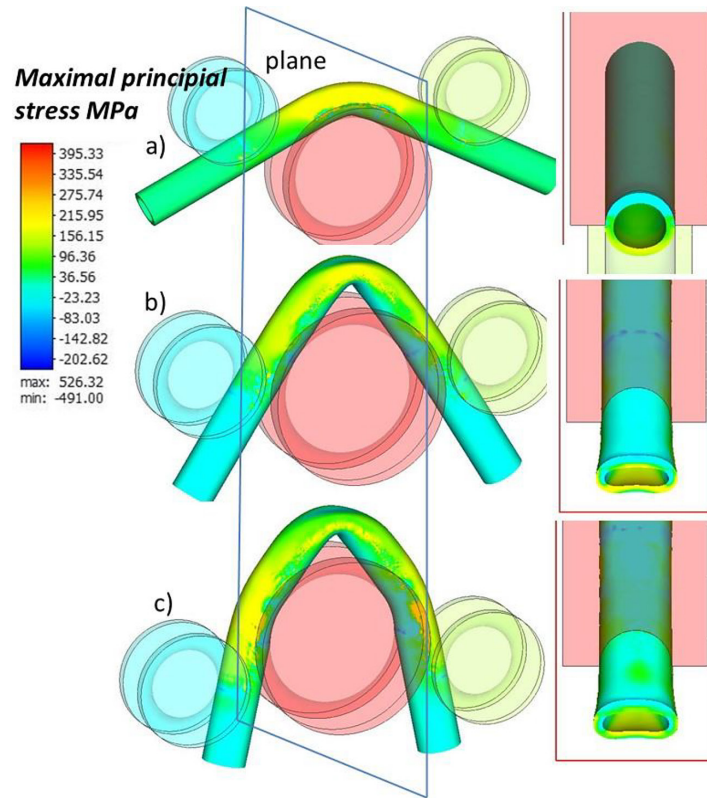


**Fig. 5.** Changes in the shape of an EN-AW 6060 aluminum alloy tube in a bending process conducted with a bending radius of  $R_g = 1.5 D_z$  and a bending angle of  $180^\circ$ , using circular bending roll impression, (a) process progress – 30%, (b) process progress – 60%, (c) process progress – 90%

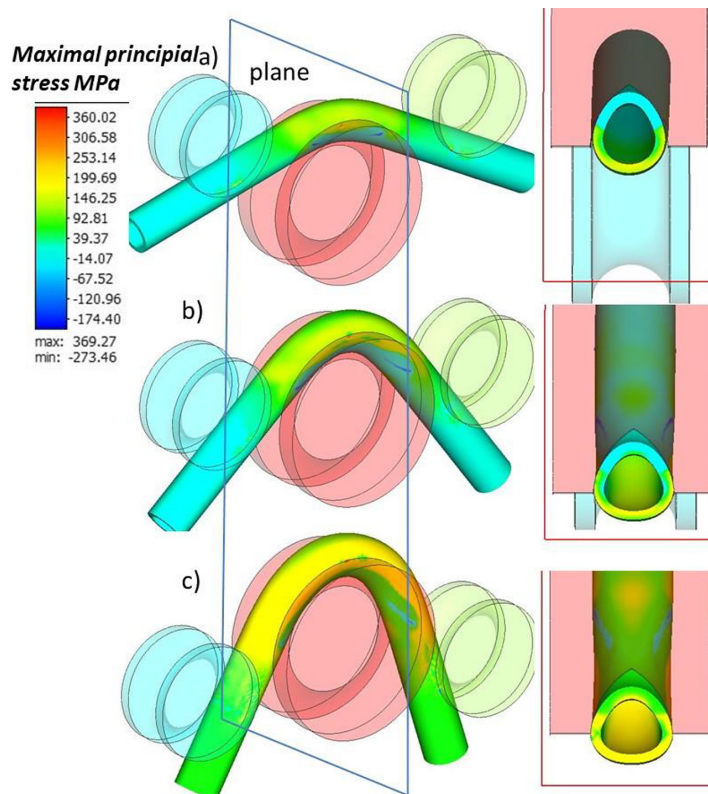


**Fig. 6.** Changes in the shape of an EN-AW 6060 aluminum alloy tube in a bending process conducted with a bending radius of  $R_g = 1.5 D_z$  and a bending angle of  $180^\circ$ , using elliptical ( $h = 2 \text{ mm}$ ) bending roll impression, (a) process progress 30%, (b) process progress 60%, (c) process progress 90%

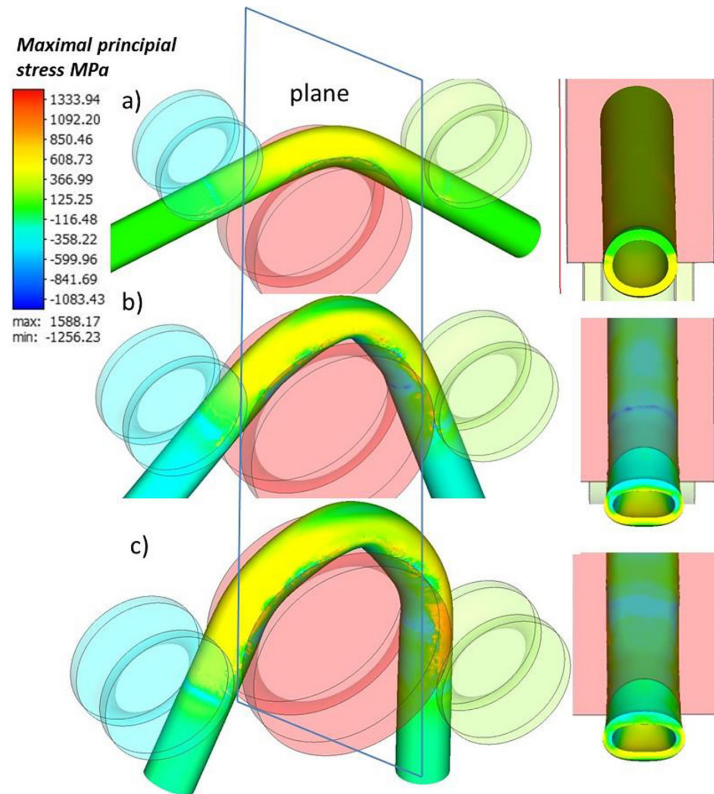


**Fig. 7.** Changes in the shape of a 16Mo3 steel tube in a bending process conducted with a bending radius of  $R_g = 1.5 D_z$  and a bending angle of  $180^\circ$ , using circular bending roll impression, (a) process progress 30%, (b) process progress 60%, (c) process progress 90%

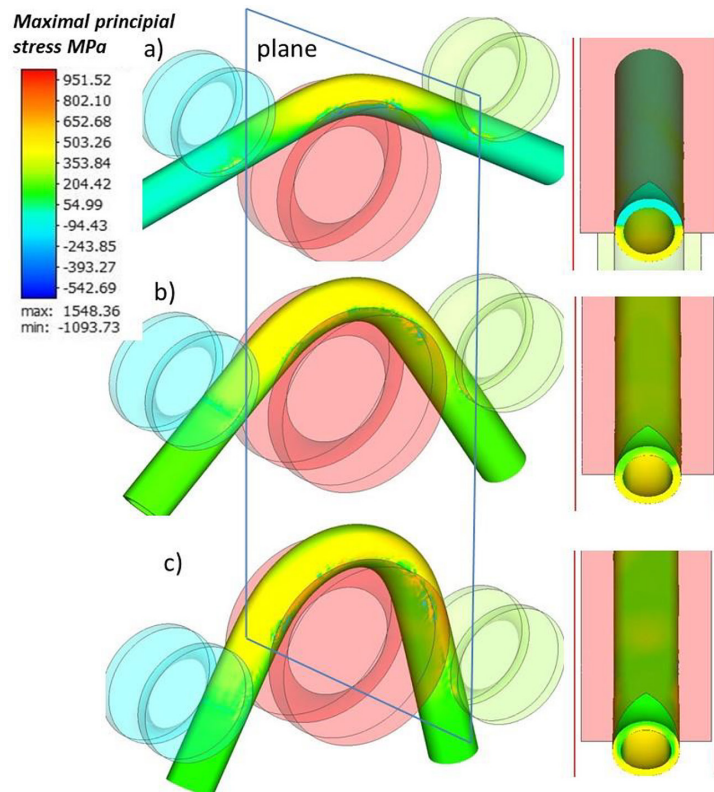


**Fig. 8.** Changes in the shape of a 16Mo3 steel tube in a bending process conducted with a bending radius of  $R_g = 1.5 D_z$  and a bending angle of  $180^\circ$ , using elliptical ( $h = 8 \text{ mm}$ ) bending roll impressions, (a) process progress 30%, (b) process progress 60%, (c) process progress 90%

led to reduced ovalization. The tube profile did not collapse and the tube wrapped around the roll (Figs. 6 a, b, c). In addition, the cross section shown in Figure 6 has a near-circular shape, which indicates that it has the desired flow capacity and low ovalization.

Figures 7 and 8 show selected numerical results of the bending process for 16Mo3 steel tubes.

The 16Mo3 steel grade has a greater deformability than the EN-AW 6060 aluminum alloy. The total elongation for 16Mo3 steel is  $A5 = 25\%$  [22] and for EN-AW 6060 aluminum alloy  $A5 = 14\%$  [21]. The circular impression used to bend the tube with a radius of  $R_g = 1.5D_z$  did not give a positive result for either material. After reaching a bending angle of about  $90^\circ$ , ovalization occurred, the degree of which was so large that it can be seen in the figures (Figs. 7b, c). The use of the elliptical impression of the bending roll (here for the variant of the bending roll impression  $h = 8$  mm) resulted in reduced ovalization. The cross section in the bending zone is more circular (Figs. 8b, c). In addition, there is no characteristic collapse in the profile as in the case of the circular impression of the bending roll (Fig. 7c).

Table 3 shows the cross sections in the bending zone for all tested variants of impression shape and a bending radius of  $R_g = 1.5D$ .

This made it possible to take into account the whole spectrum of the examined variants of bending roll impressions and make a comparative analysis. As it can be seen from the cross sections of bent tubes listed in Table 3, the insertion depth of the profile for steel and aluminum alloy caused different ovalization effects. A visual assessment made it possible to conclude that for the 16Mo3 steel grade, the use of the circular impression with  $h = 10$  mm caused a pronounced ovalization of the cross section in the bending zone during bending. Visually, the use of other variants of elliptical impression did not cause the ovalization effect. For the EN-AW 6060 aluminum alloy sample, the use of the circular impression of the bending roll ( $h = 10$  mm) and the elliptical impression ( $h = 8$  mm) resulted in the flattening of the cross section. In contrast, for other cases, the obtained cross sections were free from significant ovalization. To determine whether the ovalization was acceptable, measurements and calculations had to be made.

The next step was a numerical determination of the ovalization parameter “e” using Formula (1).

Figures 9 and 10 show the results of minimum and maximum diameters measured to determine the ovalization of bent tube cross sections for EN-AW 6060 aluminum alloy and 16Mo3 steel, respectively.

**Table 3.** Values of the cross section of bent tubes at different stages of the process (20, 50, 75, 100%)

EN-AW 6060					16Mo3				
Bending radius $R_g = 1.5D$					Bending radius $R_g = 1.5D$				
h, mm	Cross section of the tube in the bending zone				h, mm	Cross section of the tube in the bending zone			
	Process progress [%]					Process progress [%]			
	25	50	75	100		25	50	75	100
10					10				
8					8				
6					6				
4					4				
2					2				

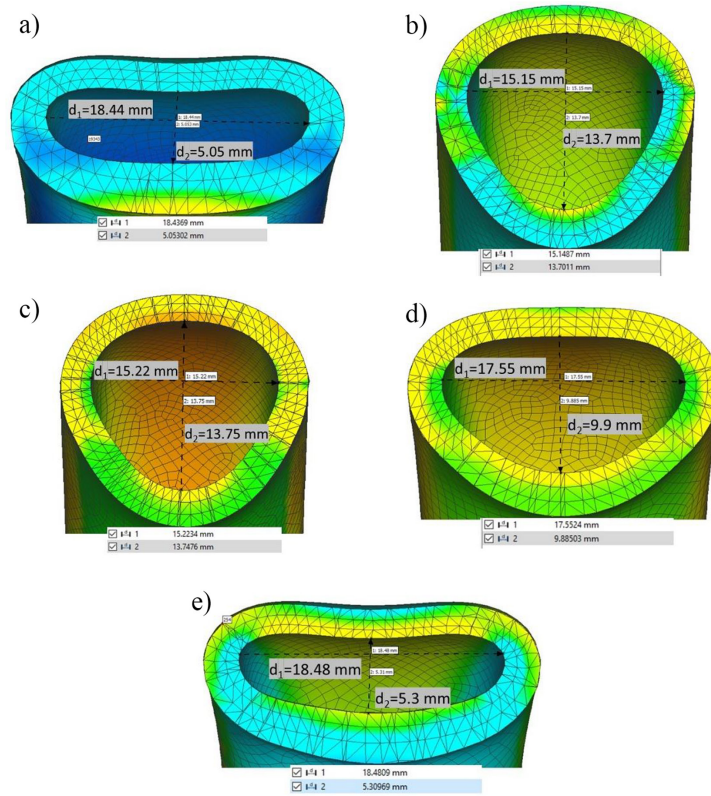


**Fig. 9.** Measurement results of the diameters in the tube cross section for a bending angle of  $\alpha = 180^\circ$  for EN-AW 6060 aluminum alloy (a) circular impression, (b) elliptical impression ( $h = 2$  mm), (c) elliptical impression ( $h = 4$  mm), (d) elliptical impression ( $h = 6$  mm), (e) elliptical impression ( $h = 8$  mm)

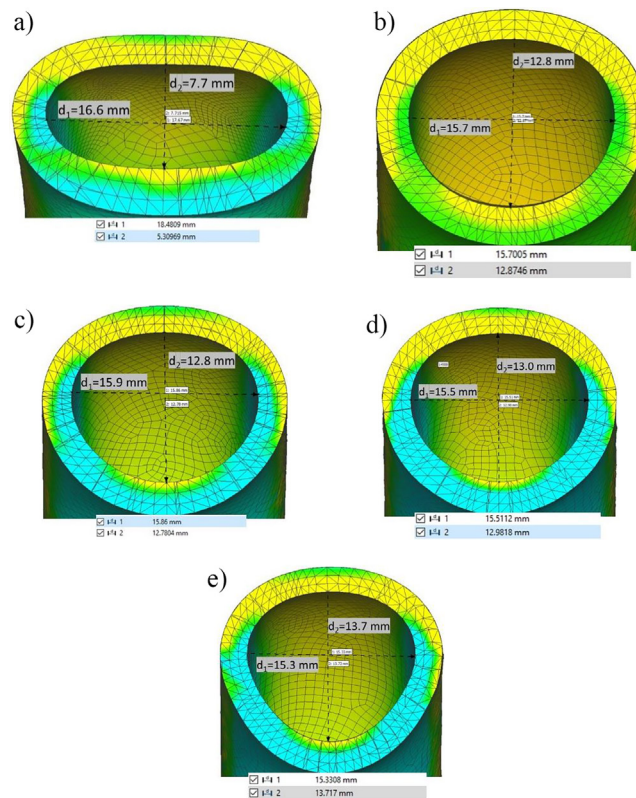


**Fig. 10.** Measurement results of diameters in the tube cross section for a bending angle of  $\alpha = 180^\circ$  for 16Mo3 steel (a) circular impression, (b) elliptical impression ( $h = 2$  mm), (c) elliptical impression ( $h = 4$  mm), (d) elliptical impression ( $h = 6$  mm), (e) elliptical impression ( $h = 8$  mm)

**Table 4.** Values of the ovalization parameter  $e$  obtained with a bending radius of  $R_g = 1.5D_z$  – numerical results

EN-AW 6060				16Mo3			
Bending radius $R_g=1.5D$				Bending radius $R_g=1.5D$			
$h$ [mm]	$D_{max}$ [mm]	$D_{min}$ [mm]	ovalization, $e$ [%]	$h$ [mm]	$D_{max}$ [mm]	$D_{min}$ [mm]	ovalization, $e$ [%]
8	18.48	5.31	55.35	8	15.33	13.7	5.55
6	17.55	9.88	27.96	6	15.51	12.98	8.87
4	15.22	13.75	5.07	4	15.86	12.78	9.88
2	15.15	13.70	5.02	2	15.77	12,875	12.75
10	18.43	5.05	56.98	10	17,67	7,715	39.2

Table 4 shows the numerical results of tube diameters and ovalization parameter “ $e$ ” determined from Equation (1) for individual roll impressions in bending tubes with small radii.

The numerical simulations of the tube bending process showed that the shape of the bending roll impression had a very significant effect on the geometry of the cross section of the profile in the bending zone. As expected, the use of the circular bending roll impression resulted in a significant flattening of the cross section of the tube. The ovalization  $e$  value of the cross section for the 16Mo3 steel sample is nearly 40% and for EN-AW 6060 aluminum alloy it exceeds 50% (Table 4). These values considerably exceed the requirements of the PN-EN 12952-5 standard, according to which for a bending radius of  $R_g = 1.5D_z$ , the value of ovalization  $e$  must not exceed 12%. For the 16Mo3 boiler steel tube, the use of the elliptical impressions with a tube insertion depth of  $h = 4$  mm, 6 mm and 8 mm resulted in ovalization values below 12%. The aluminum alloy tube bent using the elliptical impressions with tube insertion depths  $h = 4$  mm and 6 mm met the requirement of the standard.

## EXPERIMENTAL

The next stage of the study involved experimental validation of the numerical results. The experiments were carried out under the laboratory conditions with the use of an electromechanically driven testing machine. For this purpose, a tool set was devised in accordance with the model shown in Figure 1.

Figure 11 shows a tool set for bending tubes with small radii in the workspace of a Zwick testing machine. Bending rolls and support rollers are the key elements in the design of this tool. Owing to their adjustment ability, the support rollers allow the use of different bending angles. The bending rolls are responsible for the bending radius and forming of a tube. The shape of the impression determines the flow of material around the circumference of the tube.

Figure 12 shows a set of bending rolls used in laboratory tests. Experiments were carried out for a bending radius of  $R_g = 1.5D_z$ . Tubes bent with this bending radius value had the greatest ovalization of the cross section. This was shown by preliminary numerical calculations.

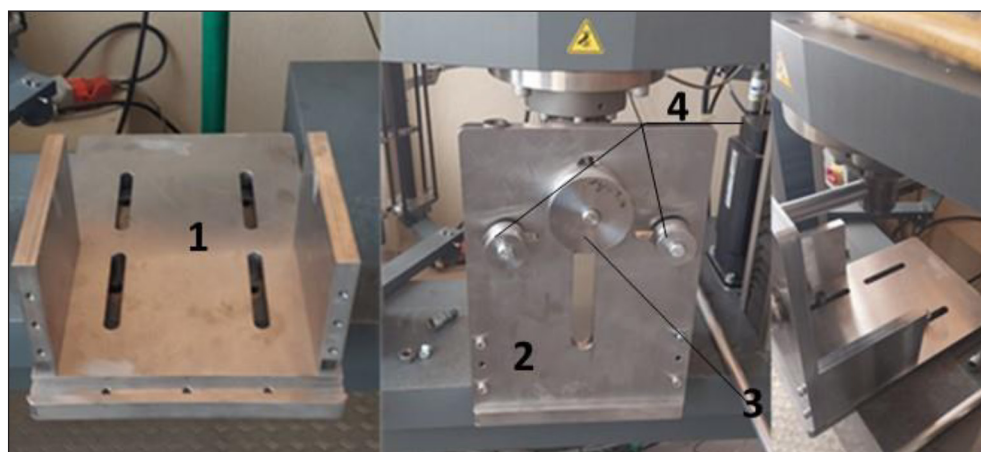


**Fig. 11.** Tool set for mandrel-free bending of tubes with small radii in the workspace of a Zwick testing machine: (1) tool base, (2) faceplate, (3) bending roller, (4) support rollers

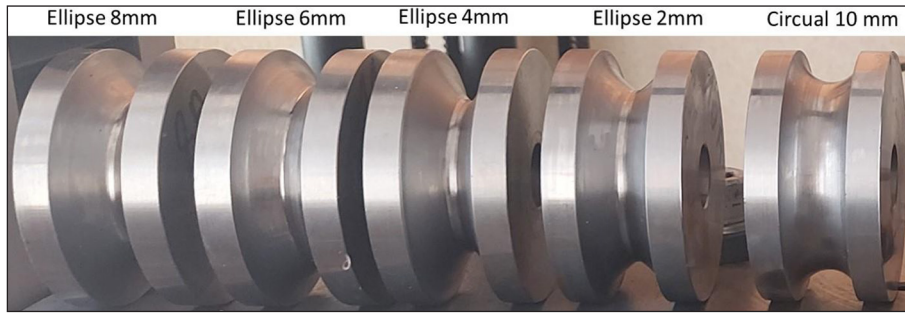


Fig. 12. Bending rolls with different impressions for tube bending conducted with a bending radius of  $R_g = 1.5D$

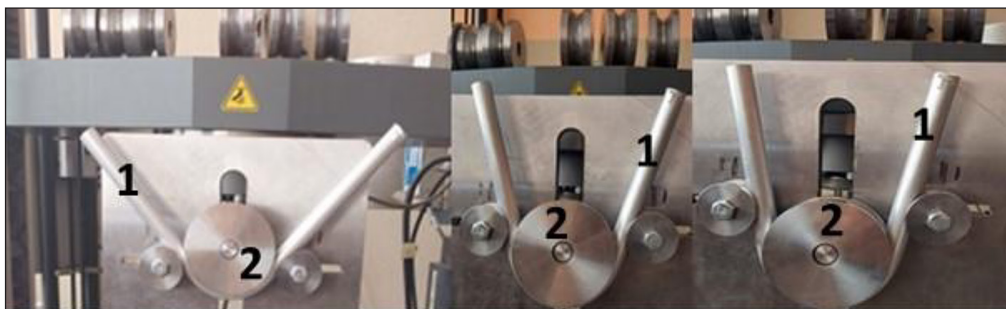


Fig. 13. Selected stages of a bending process for EN-AW 6060 aluminum alloy tubes, conducted with a bending angle of  $\alpha = 180^\circ$  and a bending radius of  $R_g = 1.5Dz$ : (1) tube in the various phases of bending, (2) bending roller

The test samples used in the experiments were the same as those used in the numerical simulations, i.e. tubes made of EN-AW 6060 aluminum alloy and 16Mo3 boiler steel, with an outside diameter of  $Dz = 20$  mm and a wall thickness of  $t = 2.0$  mm.

Figure 13 shows selected stages of the bending process for tubes made of the EN-AW 6060 aluminum alloy.

Figure 14 shows the experimental results obtained for an aluminum alloy tube bent using a circular roll impression.

The results of the bending tests clearly demonstrate that the bending radius  $R_g = 1.5Dz$  in combination with the circular impression results in the

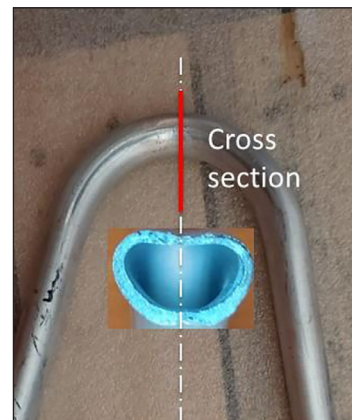


Fig. 14. EN-AW 6060 aluminum alloy tube after a bending process conducted with a bending radius of  $R_g = 1.5Dz$

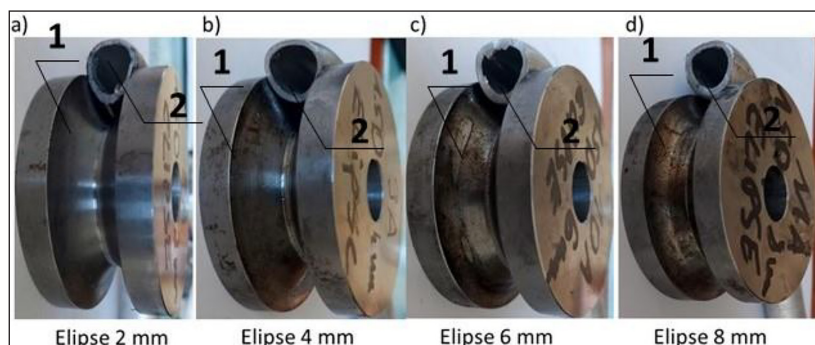
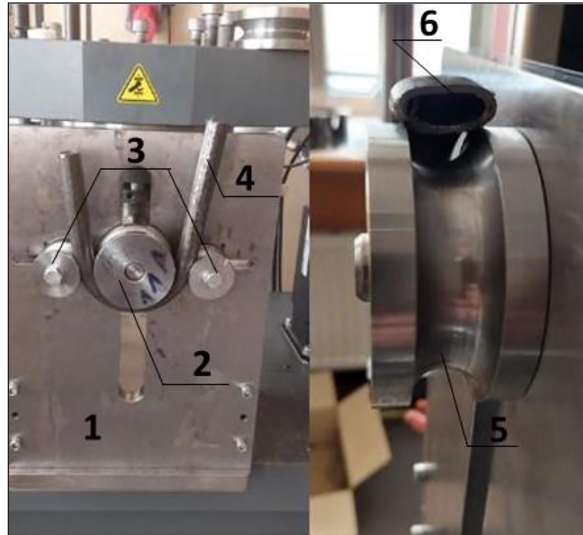


Fig. 15. Results of a tube bending process conducted with a bending radius of  $R_g = 1.5Dz$  using elliptical impressions, with a tube insertion depth  $h$  of: (a) 2 mm, (b) 4 mm, (c) 6 mm, (d) 8 mm – for EN-AW 6060 aluminum alloy. 1 – view roll shape of roll pass, 2 – bent tube in section

flattening of the tube cross section. The cross section is oval and the top wall of the tube has collapsed.

Figures 15 a–d show the cross sections of EN-AW 6060 aluminum alloy tubes in the bending zone for all tested variants of bending rolls with non-circular (elliptical) impressions. It can



**Fig. 16.** Tube and its cross section after a bending process conducted using a circular impression, with a bending radius of  $R_g = 1.5D_z$  – for 16Mo3 steel, (1) faceplate, (2) bending roller, (3) support rollers, (4) bent tube, (5) view roll shape of roll pass, bent tube in section

be observed that the obtained cross sections are of higher quality than the cross sections obtained in the bending process conducted with a circular bending roll impression.

Experiments were also performed for the 16Mo3 boiler steel tube. Figure 16 presents the tube with a diameter of  $D_z = 20$  mm and a wall thickness of  $t = 2$  mm, and its cross section after the bending process conducted using a circular impression, with a bending radius of  $R_g = 1.5D$ .

Figures 17 a–d show the cross sections of 16Mo3 steel tubes in the bending zone, obtained with elliptical bending roll impressions.

Like in the theoretical part, the cross sections of the bent tubes made of both material grades were measured at the cross section with the greatest deformation. Based on the minimum and maximum inside diameters, the ovalization  $e$  was calculated. Obtained experimental are listed in Table 5.

## DISCUSSION OF THE RESULTS

The purpose of the study was to determine the optimal geometric parameters of bending roll impressions. The criterion was to achieve the lowest degree of ovalization of the tube cross section in the bending zone.

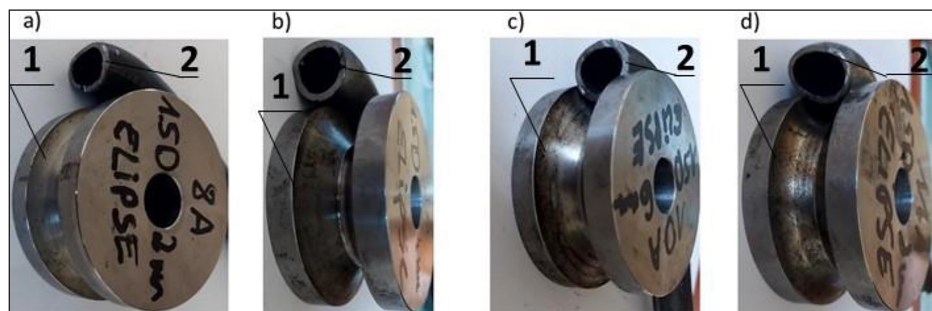


**Fig. 17.** Results of a tube bending process conducted with a bending radius of  $R_g = 1.5D_z$  using elliptical impressions, for a tube insertion depth  $h$  of: (a) 2 mm, (b) 4 mm, (c) 6 mm, (d) 8 mm – for 16Mo3 steel, (1) view roll shape of roll pass, (2) bent tube in section

**Table 5.** Values of the ovalization parameter  $e$  obtained with a bending radius of  $R_g = 1.5D_z$  - experimental results

AW-EN 6060				16Mo3			
Bending radius $R_g = 1.5D$				Bending radius $R_g = 1.5D$			
$h$ [mm]	$D_{max}$ [mm]	$D_{min}$ [mm]	ovalization, $e$ [%]	$h$ [mm]	$D_{max}$ [mm]	$D_{min}$ [mm]	ovalization, $e$ [%]
8	18.22	5.52	53.49	8	15.51	13.7	6.19
6	18.01	10.50	26.34	6	15.77	13.19	8.90
4	14.99	13.25	6.16	4	15.80	12.51	11.60
2	15.51	13.33	5.55	2	16.10	12.55	12.39
10	18.05	5.21	55.20	10	17.49	7.20	41.67

A circular bending roll impression was the first tested shape used in the experimental mandrel-free tube bending. The numerical simulations showed that when the EN-AW 6060 aluminum alloy tube was bent with a bending radius of  $R_g = 1.5D$  using the circular tool with  $h = 10$  mm, the material cracked or collapsed, and the ovalization degree was 56.98%. The experiment confirmed the results of the computer simulations for this case of the bending roll impression, and the experimentally obtained ovalization value was 55.20%. Similarly, the results of the numerical calculations agreed with the experimental findings obtained for the 16Mo3 boiler steel tube. The ovalization obtained in the computer simulation

for  $h = 10$  mm amounted to 39.2% and in the experiment to 41.64%. These values significantly exceed the acceptable ovalization value of 12%.

Figures 18 and 19 show a comparison of the theoretical and experimental results in terms of the relationship between ovalization  $e$  and depth  $h$  for the EN-AW 6060 aluminum alloy and 16Mo3 steel tubes, respectively. The comparison reveals high agreement between the numerical and experimental results for both material grades. The plots also indicate the limit value of ovalization  $e$  (equal to 12%) as specified by the PN-EN 12952-5 standard.

For the EN-AW 6060 aluminum alloy tube (Fig. 18), the minimum value of ovalization is obtained with  $h = 2$  mm, while the requirement of

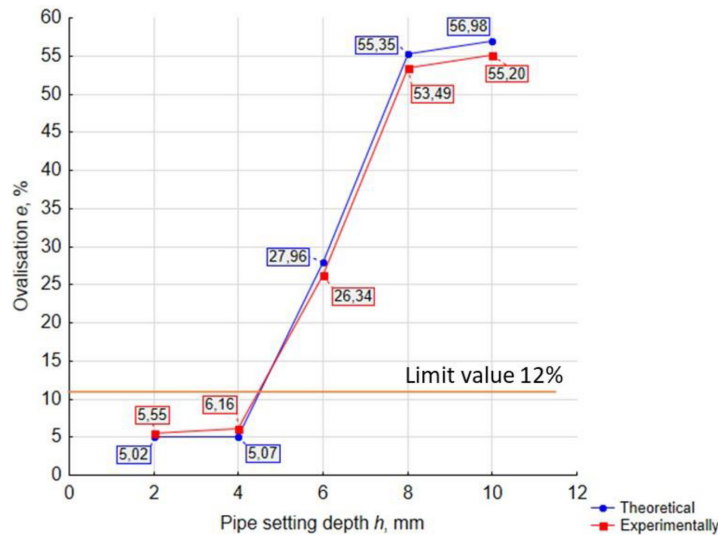


Fig. 18. Ovalization  $e$  versus tube insertion depth  $h$  for EN-AW 6060 aluminum alloy – a comparison of the theoretical and experimental result

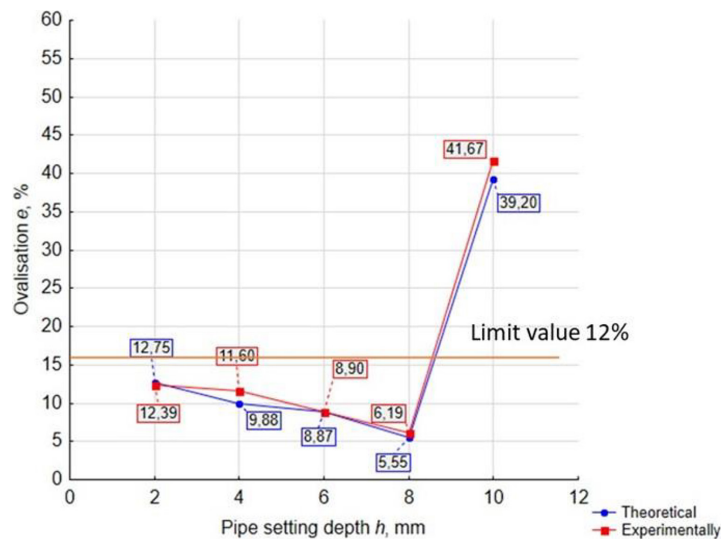


Fig. 19. Ovalization  $e$  versus tube insertion depth  $h$  for 16Mo3 steel – a comparison of the theoretical and experimental results

the standard are met when the impressions with  $h = 2$  mm and  $h = 4$  mm are used. Bending conducted using other impression shapes results in a greater ovalization degree than acceptable under the standard.

For the 16Mo3 steel tube (Fig. 19), the minimum value of ovalization is obtained with  $h = 8$  mm, while the requirements of the standard are met when the impressions with  $h = 4$  mm,  $h = 6$  mm and  $h = 8$  mm are used. Bending conducted using other impressions results in a greater ovalization degree than acceptable under the standard.

In the experiments, the degree of cross-sectional ovalization in the bending zone was also assessed using a check ball. This method is described in the PN-EN 12952-5 standard. The check ball was printed from ABS polymer using a 3D printer. In accordance with the PN-EN 12952-5 standard, the diameter of the check ball was  $0.86D_w$ , where  $D_w$  is the inside diameter of the

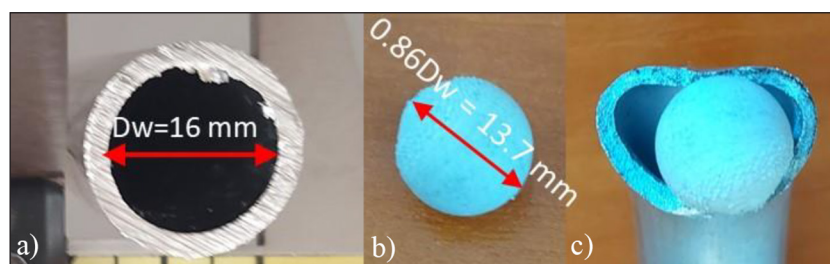
tube. If the ball can pass freely through the hole in the bending zone, this means that the ovalization is within the acceptable range.

Figure 20 shows an example of using a check ball for determining the degree of cross-sectional ovalization after a bending process conducted with a circular impression tool.

As demonstrated by the test results in Figure 20c, the diameter of the check ball was much larger than the diameter of the tube after bending. Consequently, the ball could not pass through the hole of the tube in the bending zone. This means that the ovalization is outside of the acceptable range.

Like in the case of the circular impression, an ovalization test with the check ball was also performed for the elliptical impressions.

Figures 21 a-d show the cross sections of the EN-AW 6060 aluminum alloy tubes in the



**Fig. 20.** Test of cross-sectional ovalization conducted with a check ball for a bending process of EN-AW 6060 aluminum alloy tubes by circular impression rolls: (a) tube before the bending process  $D_w = 16$  mm, (b) check ball with a diameter of  $0.86D_w = 13.7$  mm, (c) tube after the bending process

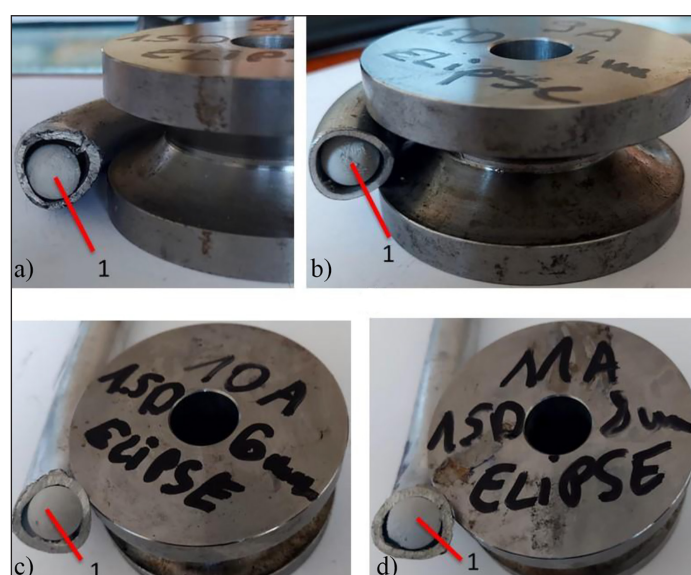


**Fig. 21.** Ovalization test conducted with a check ball on EN-AW 6060 aluminum alloy tubes bent using elliptical impressions, for a tube insertion depth  $h$  of: (a) 2 mm, (b) 4 mm, (c) 6 mm, (d) 8 mm and a bending radius of  $R_g = 1.5D_z$ , 1 – check ball

bending zone during the test of passing a check ball through the hole.

The experimental results obtained for the EN-AW 6060 aluminum alloy tubes show high agreement with the results of the theoretical calculations. The simulations of bending tubes with small radii showed that the ovalization of the cross section met the conditions of the standard when the process was conducted using the elliptical impressions with a tube insertion depth of  $h = 4$  and  $8$  mm (Table 4). The ovalization of the cross section in the bending zone did not exceed 12%. The check ball with a diameter of  $0.86D_w$  could be freely passed through the hole in the bending zone, as shown in Figure 21 and Table 5. In contrast, the elliptical impressions with a tube insertion depth of  $h = 6, 8$  and  $10$  mm produced such a high percentage degree of ovalization that the check ball could not pass through the hole of the tube in the bending zone. These results agree with the numerical results listed in Table 3.

For the bending process of a 16Mo3 steel tube in a circular impression, a significant degree of ovalization of the cross section was also observed. To validate this observation experimentally, an ovalization test was performed using a check ball with a diameter of  $0.86$  of the tube inside diameter. Figure 22 shows the check ball

against the tube cross section in the bending zone for the tool with a circular impression.

Figures 23 a-d show the cross sections of the 16Mo3 steel tubes in the bending zone obtained for the bending process conducted using elliptical roll impressions, and the test of driving a check ball through the tube hole.

The experimental results of bending 16Mo3 boiler steel tubes with small radii show high agreement with the results of the theoretical calculations. The computer simulations of tube bending using small radii showed that the cross sectional ovalization satisfied the standard requirements when the elliptical impressions with tube insertion depths of  $h = 4, 6$  and  $8$  mm were used (Table 4).

The ovalization of the cross section in the bending zone did not exceed 12%. The check ball with a diameter of  $0.86D_w$  could freely pass through the hole in the bending zone. On the other hand, the bending process conducted using the impressions with a tube insertion depth of  $h = 2$  and  $10$  mm resulted in such a high percentage degree of ovalization that the check ball could not pass through the tube hole in the bending zone. These results confirm the results obtained for 16Mo3 steel listed in Table 5.

## CONCLUSIONS

This paper presented the numerical and experimental results of a study investigating a tube bending process conducted with a bending angle of  $180^\circ$  and a bending radius of  $R_g = 1.5D_z$ . The numerical analysis and the experiments were performed under the same bending conditions. The bending process involved three-point bending of the tube to obtain a “U” shape. The study was performed on tubes made of EN-AW6060 aluminum alloy and 16Mo3 boiler steel. All tubes had a diameter of  $20$  mm and a wall thickness of  $2$  mm.

The results of the study lead to the following conclusions. For the EN-AW 6060 aluminum alloy and 16Mo3 boiler steel samples, the use of



Fig. 22. Ovalization test conducted with a check ball on 16Mo3 steel tubes bent using a circular impression, (1) check ball with a diameter of  $0.86D_w = 13.7$  mm

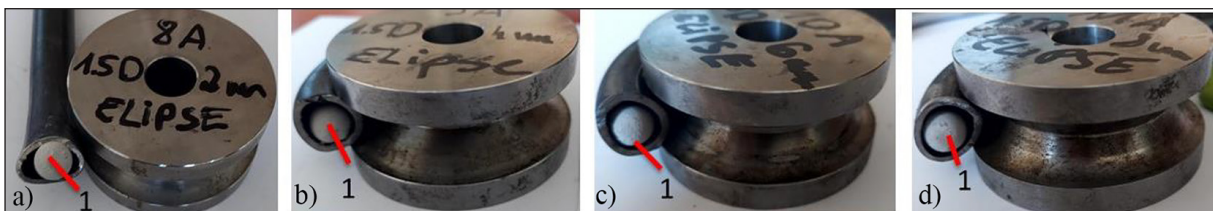


Fig. 23. Ovalization test conducted with a check ball on 16Mo3 steel tubes bent using elliptical impressions, for a tube insertion depth  $h$  of: (a)  $2$  mm, (b)  $4$  mm, (c)  $6$  mm, (d)  $8$  mm, and a bending radius of  $R_g = 1.5D_z$ , 1 – check ball

circular impressions in the bending rolls resulted in large values of the degree of cross-sectional ovalization. The values of the ovalization parameter  $e$  were close to 60% for the aluminum alloy sample and to 40% for the steel sample. The tubes completely lost their flow capacity and stability. For the EN-AW 6060 aluminum alloy sample, the use of the elliptical impressions with two tube insertion depths  $h$  of 6 and 8 mm resulted in reduced cross-sectional ovalization. The decrease was negligible and the ovalization values exceeded 12%. The use of the elliptical impressions with the tube insertion depths  $h$  of 2 and 4 mm yielded very satisfactory results and the values of the ovalization parameter  $e$  were slightly above 5%. For the 16Mo3 boiler steel sample, the use of the elliptical impression with a tube insertion depth of  $h = 2$  mm caused a visible decrease in cross-sectional ovalization. The ovalization values were above 12%. The use of the elliptical impressions with three different tube insertion depths  $h$  of 4, 6 and 8 mm produced very satisfactory results, with the  $e$  parameter values below 12%. The experimental findings showed agreement with the numerical results. For the bending roll impressions where the numerical calculations showed that the  $e$  parameter was greater than 12%, the experiments revealed that the check ball did not pass through the hole of the tube in the bending zone. The cross section did not meet the requirements of the standard. The numerical and experimental results showed that tube bending conducted using different roll impressions had different effects on the tested aluminum alloy and steel samples. Each material deformed in a different manner. Since the 16Mo3 steel grade is more deformable (elongation  $A5 = 24\%$ ), the steel tube had to be inserted deeper into the impression, so that the cross section did not collapse or flatten. Aluminum alloy is more reinforced and less deformable (elongation  $A5 = 15\%$ ), so the applied insertion depth in the impression limited the flow of the material around the circumference, and the cross section collapsed from the top and flattened. Therefore, it can be concluded that for each type of material, the tube insertion depth  $h$  in the impression must be determined individually in order to reduce as much as possible the number of defects in the cross section.

## REFERENCES

1. Misiūnaitė I., Rimkus A., Jakuboskis R., Sokołow A., Gribniak W. Analysis of local deformation effects in cold-formed tubular profiles subjected to

- bending. *Journal of Constructional Steel Research*. 2019; 160: 598–612.
2. Asnafi N., Nilsson T., Lassel G. Automotive Tube Bending and Tubular Hydroforming with Extruded Aluminium Profiles. *Journal Of Materials & Manufacturing*. 2000; 109: 919–933.
3. Vatter P.H., Plettke R. Process Model for the Design of Bent 3-Dimensional Free-Form Geometries for the Three-Roll-Push-Bending Process. *Procedia CIRP*. 2013; 7: 240–245.
4. Ghiotti A., Simonetto E., Bruschi S., Bariani P. F.Springback measurement in three roll push bending process of hollow structural sections. *CIRP Annals - Manufacturing Technology*. 2017; 66(1): 289–292.
5. Chung Y.J., Barlat F., Lee M. Bending Formability of Ferritic Stainless Steels for Application to Tubular Exhaust. *Manifolds International*. 2015; 55(1): 1048–1057.
6. Hermes M., Staupendahl D., Becker Ch., Erman Tekkaya A. Innovative Machine Concepts for 3D Bending of Tubes and Profiles. *Key Engineering Materials*. 2011; 473: 37–42.
7. Zhan M., Wang Y., Yang H., Long H. An Analytic Model for Tube Bending Springback Considering Different Parameter Variations of Ti-Alloy Tubes. *Journal of Materials Processing Technology*. 2016; 236: 123–137.
8. Li H., Yang H., Song F., Zhan M. Springback Characterization and Behaviors of High-Strength Ti–3Al–2.5 V Tube in Cold Rotary Draw Bending. *Journal of Material Processing Technology*. 2012; 9: 1973–1987.
9. Al-Qureshi H.A. Elastic-Plastic Analysis of Tube Bending. *International Journal of Machine Tools and Manufacture*. 1999; 39(1): 87–104
10. Xunzhong G., Hao X., Yong X., Yannan M., Ali A.E., Jie T., Kai J. Free-bending process characteristics and forming process design of copper tubular components. *The International Journal of Advanced Manufacturing Technology*. 2018; 96: 3585–3601.
11. Simonetto E., Ghiotti A., Bruschi S. Feasibility of Motion-Capture Techniques Applied to Tube Bending. *Key Engineering Materials*. 2015; 651–653: 1128–1133.
12. Engel B., Kersten S. Analytical Models to Improve the Three-Roll-Push Bending Process of Tube-Profiles. *Steel Research International Special Edition 10th ICTP 2011*; 355–360.
13. Taheri E., Firouzianhaji A., Mehrabi P., Vosough B., Samali H. B. Experimental and Numerical Investigation of a Method for Strengthening Cold-Formed Steel Profiles in Bending. *Appl. Sci*. 2020; 10: 3855
14. Hermes M., Staupendahl D., Becker C., Tekkaya A.E., Staupendahl D. Innovative machine concepts

- for 3D bending of profiles and tubes. *Key Eng Mater.* 2011; 473: 37–42.
15. Gantner P., Harrison D.K., De Silva A.K., Bauer H. The development of a simulation model and the determination of the die control data for the free-bending technique. *Proc Inst Mech Eng B J Eng Manuf.* 2007; 221: 163–171.
16. Heng L., Shi K.P., Yang H., Tian Y.L. Springback law of thinwalled 6061-t4 al-alloy tube upon bending. *Trans Nonferrous Metals Soc China.* 2012; 22(2): 357–363.
17. Djamaluddin F., Abdullah S., Ariffin A.K., Nopiah Z.M. Non-linear finite element analysis of bitubal circular tubes for progressive and bending collapses. *International Journal of Mechanical Sciences.* 2015: 99: 228-236.
18. Yang H., Heng L., Zhiyong Z., Mei Z., Jing L., Guangjun L. *Advances and Trends on Tube Bending Forming Technologies.* Chinese Journal of Aeronautics. 2012; 25: 1–12.
19. Michalczyk J. Wojsyk. K., Development and Modelling of the Method of Mandrelless Small-Radius Tube Bending. *Archives of Metallurgy and Materials.* 2015; 60: 2791-2797.
20. [https://emetal.eu/aluminium/aluminium-EN-AW-6060-ISO\\_-AlMgSi-EN\\_-AW-AlMgSi-PN\\_-PA-38-DIN\\_-AlMgSi0,5-wnr\\_-3.3206/](https://emetal.eu/aluminium/aluminium-EN-AW-6060-ISO_-AlMgSi-EN_-AW-AlMgSi-PN_-PA-38-DIN_-AlMgSi0,5-wnr_-3.3206/)
21. <http://www.mistal.pl/2013-03-26-17-30-34/rury-do-zastosowan-cisnieniowych-w-podwyszonych-temperaturach-rury-kotlowe-pn-en10216-2-din-17175>
22. Wojsyk K., Wrona T. A method for pinless tube bending. *Advances in Metal Forming.* Association of Mechanical Engineers and Technicians. (Metoda beztrzcieniowego gięcia rur. Postęp w obróbce Plastycznej Metali. Stowarzyszenie Inżynierów i Techników Mechaników). Częstochowa 1986; 37–42.